Journal of Genetic and Environmental Resources Conservation, 2017, 5(1):6-23.
www.jgerc.com Print ISSN: 2306-8663, Online ISSN: 2306 – 8280

Plants extracts as green synthesis of zirconium oxide nanoparticles

Raghad DH. Abdul Jalill[1]*, Maryam M.H.M. Jawad[2] and Ahmed N. Abd[3]

[1,2]Dep. of Biology and [3]Dep. of Physics, College of Science, University of Al-Mustainsiriyah, Baghdad, Iraq, Postal codes: 10052.
*Corresponding author: stru@uomustansiriyah.edu.iq, raghadalshybany@ymail.com

Abstract

The objective of this study was green synthesis of zirconium oxide nanoparticles (ZrO2 NPs) using different plants extracts: *Capsicum annum*, *Allium cepa* and *Lycopersicon esculentum* and Characterization of them. The results found that all NPs were in Nano size with good properties. All crystals shapes were Baddeleyite. NPs was produce by *C. annum*, their properties according to method one and method two were: average size were 100.25 nm, 86.66 nm, Roughness average (Ra) 1.17 nm and 1.08 nm, Root mean square (Sq) 1.98 nm, 1.25 nm. Crystals size were also calculate by Scherer's equation, it were 22.029 nm and 13.069 nm, optical band gaps were 5.1 eV and 5.25 eV. and according SEM, particles size were (<105, 100) nm respectively. NPs produce by *A. cepa*, their properties according to method one and method two were: average size were 105.14 nm, 83.00 nm, (Ra) was 0.238 nm and 1.09 nm , (Sq) was 0.272 nm and 1.27 nm. Crystals size were were 11.039 nm and 21.97 nm, optical band gaps were 5.3 eV and 3.9 eV and according SEM, particles size were (>80, >90) nm respectively. NPs produce by *L. esculentum*, their properties according to method one and method two were: average sizes were 94.95 nm, 95.48 nm, (Ra) was 0.509 nm and 0.427 nm, (Sq) was 0.591 nm, 0.502 nm. Crystals size were 21.370nm and 20.489 nm, optical band gaps were 5 eV and 3.4 eV and according SEM, particles size were (>80, >90) nm respectively. Both of green synthetic and standard NPs of ZrO2 had good antifungal and antibacterial activity compared with bulk particles. NPs had negative effects on plant seeds germinations and other growth parameters of B. vulgaris and E. sativa such as reductions in GP, MGT, MDG, GV and PI but they increased GR.

Keywords: *Allium cepa*; Antibacterial; *Capsicum annum*; green synthesis; *Lycopersicon esculentum*; nanoparticles; plant; ZrO_2.

Introduction

Nanotechnology is the term used to cover the design, construction and utilization of functional structures with at least one characteristic dimension measured in nanometres. It is a young and burgeoning field that encompasses nearly every discipline of science and biology. This field is defined primarily by a unit of length, the nanometer at which lies the ultimate control over the form and function of matter (Kelsall *et al.,* 2005). Different processes are used to synthesize metal nanoparticles with control down to the level of individual atoms and molecules. They used the physical approach (from top to bottom) and chemical (from bottom to top) operations. They are usually expensive, labor-intensive, non-environmentally friendly and it has toxic effects (Seabra and Durán 2015).

Modern methods has introduced to the manufacturing, made high quality nanomaterials can be achieved through a simple green synthesis compared with the artificial roads nanoparticle traditional filigree, would assist to remove ruthless processing conditions, by allowing the synthesis at physiological pH, temperature, pressure and low cost, (Ingale and Chaudhari, 2013). These simple process include the use of bacteria (Plaza *et al.,* 2016), fungi (Kalyani *et al.,* 2016), yeast, (Eugenio *et al.,* 2016), plants (Abdul Jalill *et al.,* 2016a), algae (Siddiqi *et al.,* 2016), diatoms (Kratošová *et al.,* 2013), and human cells, (El-Said *et al.,* 2014). They are safe for the environment with low cytotoxicity levels, inexpensive and high-impact effectively.

Recently, increasing interest in the use of plants (plant extracts and plants tissue cutlers) in the manufacturing over other biological systems. The low cost of cultivation, short production time, safety and the ability to up production volumes make plants an attractive platform for nanoparticle synthesis (Njagi *et al.,* 2011). In addition, it is easily available, safe to handle and contain a broad viability of metabolites and phytochemicals (ketones,

aldehydes amides, terpenoids, flavones…. etc.), (Suresh *et al.,* 2010).

Studies have shown that plants have the ability to reduce metal ions both on the surface and in various organs and tissues after penetrating ion site, (Especially those that have a high potential for reduction of metals hyperaccumulating). For example, study of Harris A.T and his colleagues show that Medicago sativa (alfalfa) and Brassica juncea (mustard greens) when grown on silver nitrate as a substrate can accumulate 50 nm silver nanoparticles to a high level (13.6% of their own weight) (Marchiol *et al.,* 2014).

Among the various metal oxide nanoparticles, zirconium oxide nanoparticles is become the most important nanoparticles in different industries because of their specific properties (high thermal and chemical stability, low thermal conductivity….etc.) such as: refractory material, cutting tools thermal barrier coating and catalyst support, (Chandra *et al.*, 2010), sensors, fuel cells, advanced ceramics, transparent and optical devices, metallic glass, (Huang *et al.*, 2011).

It is good antimicrobial agents such as *Staphylococcus aureus* and *Escherichia coli* bacterial pathogens and antifungal activity against *Candida albicans* and *Aspergillus niger* in terms of safety, durability and heat resistance when compared with conventional organic antibacterial agents, (De *et al.,* 2010; Joshi *et al*., 2010). Recently, bio-manufacturing of ZrO2 NPs had made by plant. In 2014 used extract of Aloe vera (Gowri *et al.,* 2014), and Azadirachta Indica, (Nimare and Koser, 2016), plants were choose to synthesis of ZrO_2 nanoparticle. There were very few studies which are use the fruits of plants in the green synthesis of zirconium NPs in the world and in Iraq. So this study aims to green synthesis of ZrO2 nanoparticles by *Capsicum annum*, *Allium cepa* and *Lycopersicon esculentum* plant extract and characterized the products to detect their physiochemical properties and biological properties.

Materials and Methods

Green synthesis of zirconium oxide nanoparticles by different plants extracts:

Plant extraction: The plant which used for green synthesis was: fruits of onions (*Allium cepa*), pepper (*Capsicum annum* L.) and tomatoes (*Lycopersicon esculentum*) were taken from local markets Baghdad/ Iraq and identified according to a taxonomic method in Herbarium of Iraqi Ministry of Health. Fifteen gram of fresh parts of: each plant was mixed with 250 ml of distal water by homogenized blender for three min. The extract was boiling for 10 min and filtered by Whatman number four filter paper. The residue was removed. The filtrate used for green synthesis of nanoparticles directly as soon as possible.

Synthesis: This was done by methods that appeared in Table (1) which optimized: the final concentrations of plant extracts and bulk particles, temperature and exposure time. Separately, plant extract was mixed with bulk particles in flask, placed in magnetic steer hot plate at 50C° with 1000rpm /second for different exposure time. The solutions allowed to cool at room temperature and repeated centrifugations at 15,000rpm for 10min. The supernatant was neglected. The precipitate formed was washed with double distilled water and then centrifuged at 1500rpm for 10min. This was repeated three times. The obtained precipitate (nanopawder) was dried at room temperature for 24hrs and characterized as described fallowing.

Table (1): Optimizations of green synthesis of zirconium oxide NPs by some plant's extracts.

Plant extracts	P.P	Methods	Quantity of P.EX. (ml)	BPs Final con. (mg/ml)	T. (C°)	Exp. (hr.)
Allium cepa	leaves	1	100	2.5	50	6
		2	50	10	50	6
Capsicum annum L	Fruits	1	100	2.5	50	5
		2	50	10	50	5
Lycopersicon esculentum	Fruits	1	100	2.5	50	5
		2	50	10	50	5

P.P: plants' parts; BNPs: green synthesis nanoparticles; P.EX.: Plant extracts; BPs: bulk particles; con.: concentrations; T.: temperature and Exp.: exposure time.

Characterization: The exact configuration of the fabricated, phase purity, structure, average particle size, morphology of crystals and distribution were measured using particle the fallowing technique: Atomic force microscopy (AFM) for Size, surface topography and granularity volume distribution of

green synthesized nanoparticles with AFM, (AA-680, Shimadzu-Japan), (characterized by Dr. Abdul Kareem Al-Samaraii Lab. Baghdad, Iraq, (Naveen *et al*., 2010).

UV–visible analysis: a Schimadzu 1601 spectrophotometer in 200–1100 nm range, (Ba-Abbad *et al*., 2012). For optical properties, transmittance measurements, absorption coefficient and determination of the gap energy ware calculated and described according (Meshram *et al.,* 2012).

X-ray diffraction: (XRD) was used to confirm the crystal structure (crystal phases and to determine the crystallite size of each Phase. XRD analysis was performed using an X-ray diffractometer with Cu-Kα crystal radiation (λ = 1.54A°)) scanning at a rate of ($5^{\circ}/min^{-1}$) for (2θ) range of (20°-70°). The diffraction peaks of samples were identified by comparison with (JCPDS-84-1286), according 2θ. The full width at half maximum (FWHM) in the XRD was used to determine the crystallite size using Scherer's equation, (Cullity, 1974), The strain value η, (Wei *et al.,* 2011), and the dislocation density δ value, (Jobst *et al.,* 2013), were, also, evaluated.

Fourier Transform Infrared Spectroscopy (FT-IR), Shemadzu, (Germany), spectrum was used to calculate the various functional groups present in ZrO_2. Scanning electron microscope (SEM), Vega Tescan (USA), in the Center of Nanotechnology and Advanced Materials/ University of Technology/ Iraq was used to were analyzed Nanoparticles.

Biological activities:

Preparations: Sterilized distilled water used to prepare different concentrations of: bulk particles (Eprui nanoparticles & microspheres company-china/ Baddeleyite crystal form with particles size > 1 µm), standard nanoparticles (Eprui nanoparticles & microspheres company-china, the supplier data were: color: white, shape: Baddeleyite crystal, particle size: 20-40 nanometer, assay 99.0%) and green synthesis of nanoparticles, which synthesis by the second method of *Capsicum annum L* plant extract. These green syntheses of nanoparticles were selected according to the results of their characterization.

Antibacterial activity: The Antibacterial activity of all nanoparticles were evaluated against two species of bacteria, which obtained from Department of Biology/ College of Science/ AL-Mustainsiriyah University/ Baghdad /Iraq, they were: Staphylococcus aureus and Escherichia coli. Different concentrations prepared from: bulk particles, standard nanoparticles and green synthesis of nanoparticles, which prepared in this research.

Dilution broth susceptibility assay used for the antimicrobial activity. Different Dilution of: bulk particles, standard nanoparticles and green synthesis of nanoparticles, which prepared in this research, were prepared to from (2/2, 2.5/1.5, 3/1) v/v of treatment/ nutrient broth. 1 mL of each dilution and 0.5 mL of each tested culture strains added to 8 mL of a nutrient broth, exposure to UV-light for one hour at 37 °C then incubated at 37 °C for 24 hrs., then seeded by streaking the surface of nutrient agar medium and incubated at 37 °C for 24 h. There was negative control and there were three replicate for each treatment.

$$R\%=[A-B]/A*100$$

Where: R is Represent the percentage of reduction of the number of colonies, A is The number of colony of bacteria in the control treatment and B is It represents the number of colony of bacteria after the transaction article nanoparticles.

Antifungal: The antifungal activities were evaluated against *F. graminearum and F. moniliform*e . PDA medium, prepared according, (Booth, 1977), supplemented with 100ppm of chloramphenicol and with different concentrations of nanoparticles. There was negative control of distill water in all experiment. All experiment has run in three replicate. Petri dishes were inoculated in the center with 4 mm of fungal plugs. Incubated at 28 ± 2°C for eight to ten days. The radials growth of the colonies measured. The percentage of inhibition of mycelial growth was calculated as the fallowing equation:

$$Inhibition\% = [(R1- R2)/R1] x100$$

Where: R1= the radius of normal growth in control plates; R2= the radius of inhibited growth.

The effect of nanoparticles on seeds germination of some plants: The seeds of two varieties of each of *Beta vulgaris var. vulgaris* and *Eruca sativa* (taken from Ministry of Science and Technology- Seed Technology Center) were soaked in different concentrations of: bulk particles, standard nanoparticles and green synthesis of nanoparticles suspensions for 72 hours. There was negative control (distill water) for all treatments. All seeds were incubating at (27±1 C°, 12 h. light: 12 h. dark). All experiments run in three replicate. The number of new germinated seeds was recorded daily. A seed was considered germinated when the radicle showed at least tw mm in length. Germination percentage, (Feizi, et.al, 2013), Germination rate (GR), (AL-Kaisi *et al.,* 2011) and mean germination time (MGT), (Feizi et.al, 2013) were calculated.

Results and Discussion

Green synthesis by *C. annum* L. plant extract:

Atomic force microscopy: The calculated ZrO_2 NPs sizes were measured using the software of the AFM. Size ranges were (45 - 105) and (45 - 120) nm with average diameter: 100.25 nm, 86.66 nm of method one and method two respectively, (Figure 1 A). Roughness average (Ra) and Root mean square (Sq) of method one was: 1.17 nm and 1.98 nm. While roughness average (Ra) and Root mean square (Sq) of method two was: 1.08 nm and 1.25 nm, respectively. (Figure 1 B, C) showed AFM topographic images of green synthesis ZrO2 nanoparticles.

Figure (2) showed the SEM images of standard synthetic ZrO_2 NPs and bulk particles. There sizes were about 40 nm compared large bulk particles with up to (2 µm). The formation of agglomerates containing spherical nano-size particles with an approximate diameter were ~105 nm of first method compared with less than 100 nm of second method. The results of FTIR spectroscopic which appear in figure (3) showed that the samples exhibited absorption peaks located near 380 (9) cm^-, 416 (12) cm^-, 580 (14) cm^- and 620(3) cm^{-1} which give an indication of presence Zr-O stretching bond.

The results of X-ray diffraction of all samples indicating that the structure were Baddeleyite crystalline.

Green synthesis NPs: The XRD pattern of first and second methods NPs showed the presence of five peaks of each of them. Strong diffraction peaks were: 27.907° (-111), 31.163° (111) and 33.879° (200) for first method and 28.196° (-111), 31.459° (111) and 24.193° (110) for second method. The average crystallite size of nanoparticles was calculated by Scherer's equation, they were 22.029 nm and 13.069 nm for first and second methods respectively.

Standard synthetic NPs: Strong diffraction peaks were: 28.157°, 31.45° and 24.029° corresponded to: (-111), (111) and (101) crystallographic planes. The average crystallite size of nanoparticles was 28.137 nm.

ulk particles: Strong diffraction peaks were: 28.243°, 31.49° and 34.159° corresponded to: (-111), (111) and (110) crystallographic planes, figure (4). Table (2) showed a summary of X-ray characterization of ZrO_2 Baddeleyite nanoparticles.

UV–visible spectral: The results of UV–visible spectral showed that the absorption spectra of green synthesis ZrO2 NPs exhibit strong absorption below 216 nm for both methods of green synthesis NPs, the same results had seen in standard synthetic NPs and bulk particles. The value of optical band gaps were about 5.1 eV and 5.25 eV for first and second methods of green synthesis NPs compared with with 5.2 eV and 5.3 eV for standard synthetic NPs and bulk particles respectively (Figure 5).

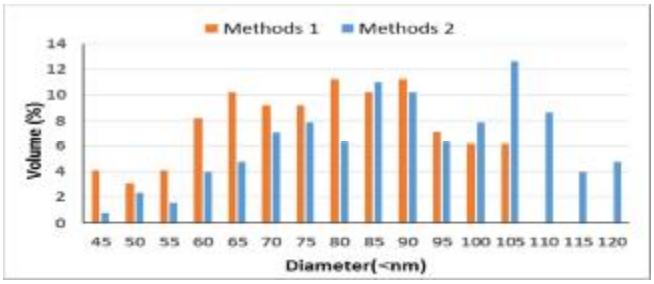

(A)

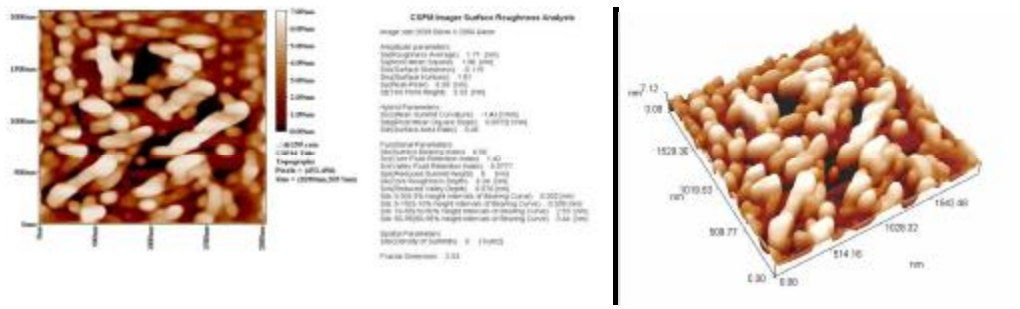

(B)

(C)

Figure (1): (A) Granularity volume distribution chart of ZrO_2 NPs synthesis by *C. annum* L plant extract using first and two methods, their average size were: 100.25 nm and 86.66 nm respectively. (B) and (C): AFM topographic images of first and two methods respectively.

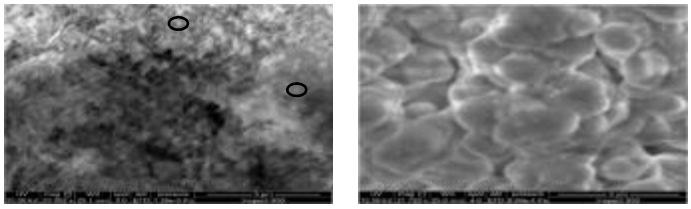

A B

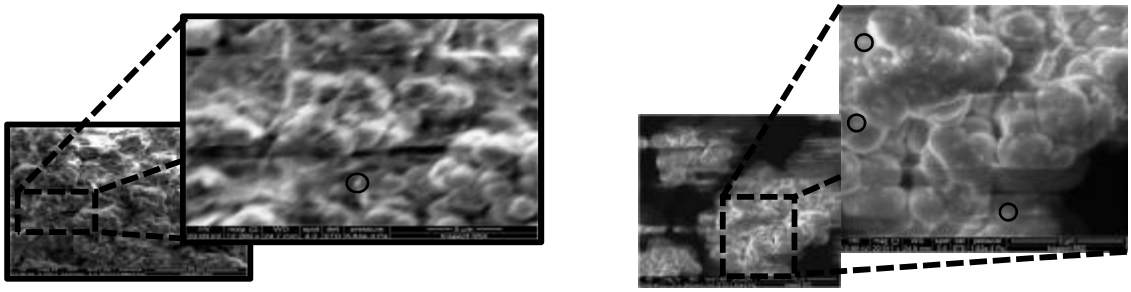

(C) (D)

Figure (2): SEM image of (A): standard synthetic nanoparticles NPs, (>40 nm), (B): bulk particles BPs, (>2 µm); ZrO_2 green synthesis NPs using: (C) first method, (<105 nm), (D) second method, (<100 nm), of *C. annum* L plant extract.

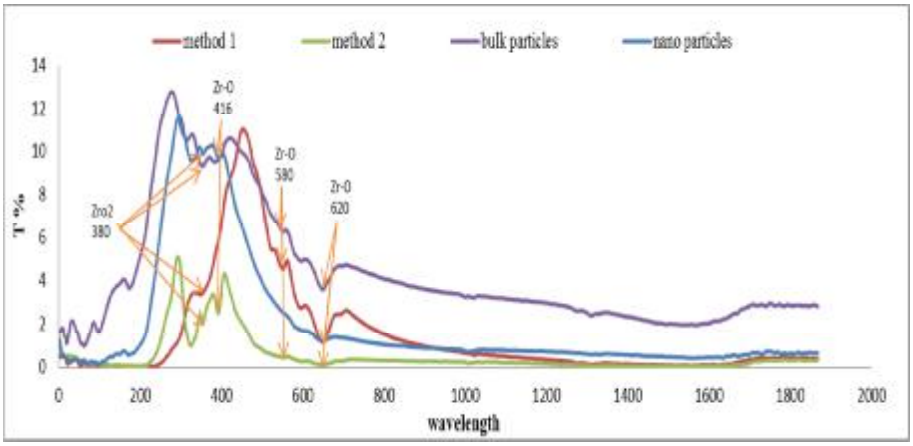

Figure (3): FT-IR spectra of ZrO_2 produced by the first and second methods *C. annum* L plant extract.

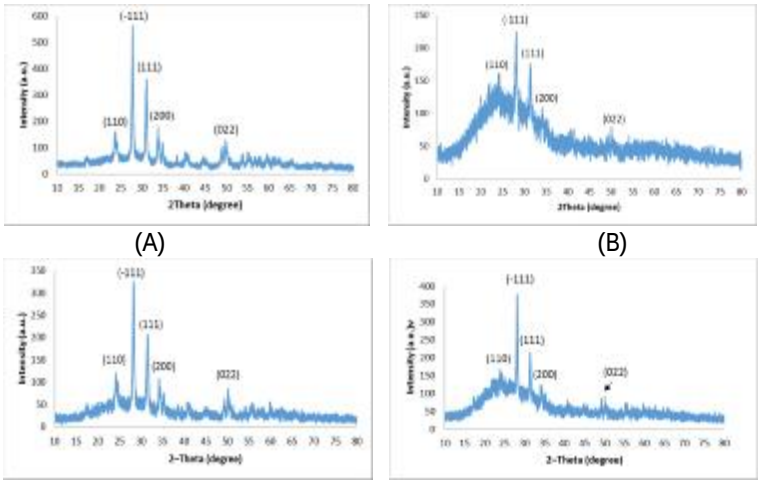

Figure (4): X-ray pattern of ZrO_2 of: (A and B) green synthesis nanoparticles using first and second methods of *C. annum* L plant extract, (C): bulk particles, (D): standard nanoparticles.

Table (2): Summary of X-ray characterization of ZrO_2 green synthesis nanoparticles synthesis by *C. annum* plant extracts compared with standard nanoparticles and bulk particles.

Sample	Planes (hkℓ)	Crystal shape	2 theta (DEG)	FWHM (DEG)	D (nm)	STRAIN XE-4	DIS X1014
Method 1	-111	Baddeleyite	27.907	0.344	23.678	58.535	17.836
	111	Baddeleyite	31.163	0.390	21.038	65.881	22.594
	200	Baddeleyite	33.879	0.387	21.372	64.851	21.893
Method 2	-111	Baddeleyite	28.196	0.553	14.724	94.133	46.127
	111	Baddeleyite	31.459	0.485	16.930	81.868	34.890
	110	Baddeleyite	24.193	1.070	7.553	183.508	175.301
standard NPs	-111	Baddeleyite	28.157	0.290	28.085	49.350	12.678
	111	Baddeleyite	31.450	0.290	28.274	49.021	12.509
	110	Baddeleyite	24.029	0.288	28.052	49.408	12.708
standard BPs	-111	Baddeleyite	28.243	0.333	24.508	56.552	16.648
	111	Baddeleyite	31.493	0.398	20.632	67.177	23.492
	200	Baddeleyite	34.159	0.233	35.427	39.123	7.968

(hkℓ) planes: crystallographic plane; FWHM : Full width at half maximum; D: dimension of Crystal in nm; η $x10^{-4}$: strain value; δ x 10^{14}: dislocation density; NPs: nanoparticles; BPs: particles.

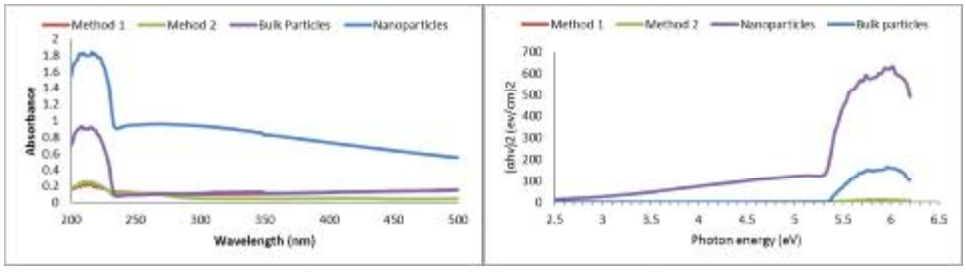

Figure (5): (A) absorptions spectrum and (B) $(ahv)^2$ versus photon energy of green synthesis ZrO_2 NPs using *C. annum* plant extract, data showed first and second methods compared with standard NPs and Bulk particles.

Green synthesis by *A. cepa* plant extract;
Atomic force microscopy: Particles size range were between (40 - 100) and (40 - 120) nm with average diameter: 105.14 nm, 83.00 nm of method first and second methods respectively. Roughness average (Ra) and Root mean square (Sq) of method one was: 0.238 nm and 0.272 nm. While roughness average (Ra) and Root mean square (Sq) of method two were: 1.09 nm and 1.27 nm, respectively. Figure (6) showed AFM topographic images of green synthesis ZrO2 nanoparticles.

The results of figure (7) showed the SEM images of ZrO_2 green synthesis NPs using first and second methods of *A. cepa*. There particle sizes were (>80 nm) and (>90 nm) of first and second methods respectively. The results of FT-IR spectra, (Figure 8), found that the samples exhibited absorption peaks located near 380(9) cm^{-1}, 519 (7) cm^{-1}, 580 (14) cm^{-1} and 620 (3) cm^{-1} which give an indication of presence Zr-O stretching bond.

The XRD pattern of first and second methods green synthesis NPs showed the presence of five peaks of each of them. Strong diffraction peaks were: 28.186° (-111), 24.123° (110) and 31.382° (111) for first method and 28.152° (-111), 31.408° (111) and 34.079° (200) for second method, (Table 3). The average crystallite sizes of nanoparticles were 11.039 nm and 21.977 nm for first and second methods respectively. The results of all samples indicating that the structure were Baddeleyite crystalline, (Figure 9).

The results of UV–visible spectral found that the absorption spectra of green synthesis ZrO_2 NPs exhibit strong absorption below 232 nm, 225 nm for first and second methods of green synthesis NPs compared with 216 in each of standard synthetic NPs and bulk particles, Figure (10). The value of optical band gaps were about 5.3 eV and 3.9 eV for first and second methods of green synthesis NPs compared with 5.2 eV and 5.3 eV for standard synthetic NPs and bulk particles respectively.

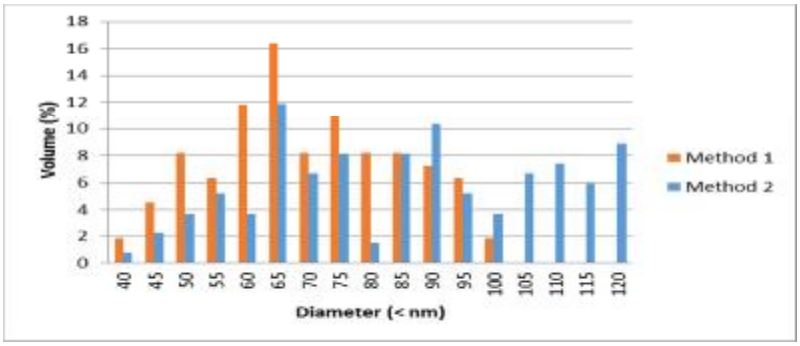

(A)

(B)

(C)

Figure (6): (A) Granularity volume distribution chart of ZrO_2 NPs synthesis by *A. cepa* plant extract using first and two methods, their average size were: 105.14 nm and 83.00 nm respectively. (B) and (C): AFM topographic images of first and two methods.

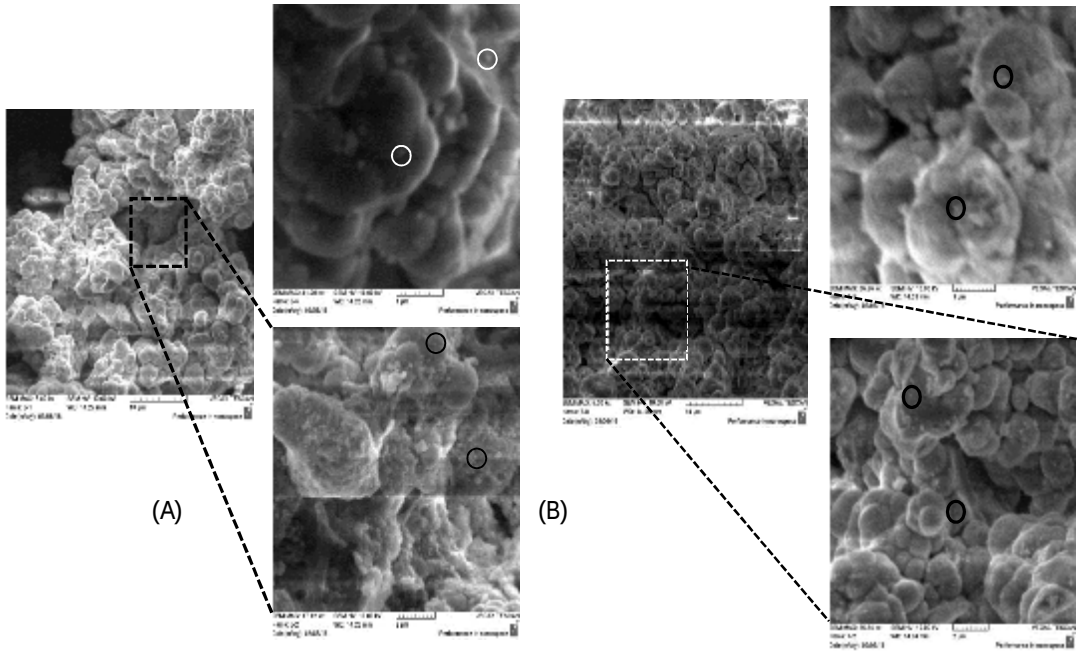

Figure (7): SEM image of ZrO_2 green synthesis NPs using: (A) first method, (>80 nm), (B) second method, (>90 nm), of *A. cepa*.

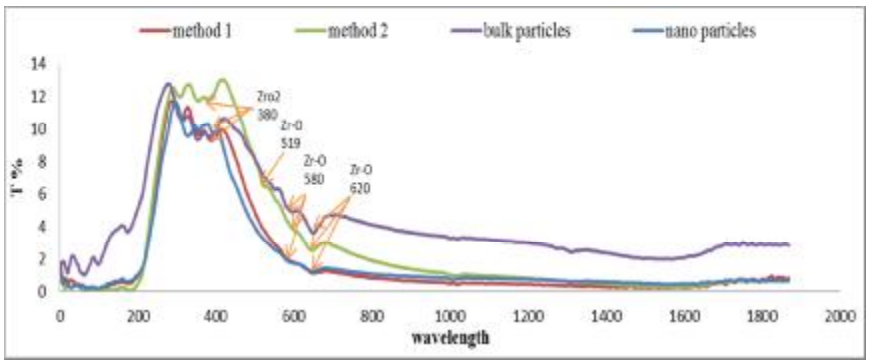

Figure (8): FT-IR spectra of ZrO_2 produced by the first and second methods *A. cepa*

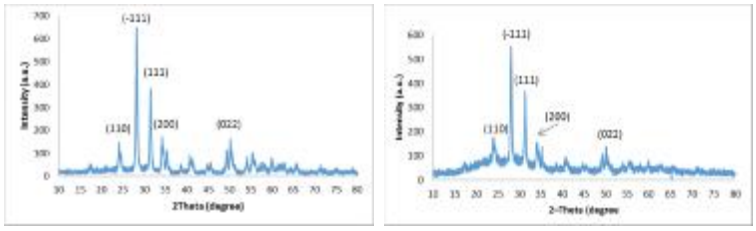

(A) (B)

Figure (9): X-ray pattern of ZrO_2 of: (A and B) green synthesis nanoparticles using first and second methods of *A. cepa* L. plant extract.

Table (3): Summary of X-ray characterization of ZrO_2 green synthesis nanoparticles synthesis by *A.cepa* plant extracts compared with standard nanoparticles and bulk particles.

Sample	Planes (hkℓ)	Crystal shape	2 theta (DEG)	FWHM (DEG)	D (nm)	STRAIN XE-4	DIS X1014
Method 1	-111	Baddeleyite	28.186	0.600	13.580	102.062	54.225
	110	Baddeleyite	24.123	1.380	5.855	236.705	291.668
	111	Baddeleyite	31.382	0.600	13.682	101.300	53.419
Method 2	-111	Baddeleyite	28.152	0.372	21.913	63.249	20.825
	111	Baddeleyite	31.408	0.383	21.419	64.710	21.798
	200	Baddeleyite	34.079	0.366	22.599	61.329	19.580

(hkℓ) planes: crystallographic plane; FWHM : Full width at half maximum; D: dimension of Crystal in nm; η x10^{-4}: strain value; δ x 10^{14}: dislocation density; NPs: nanoparticles; BPs: particles.

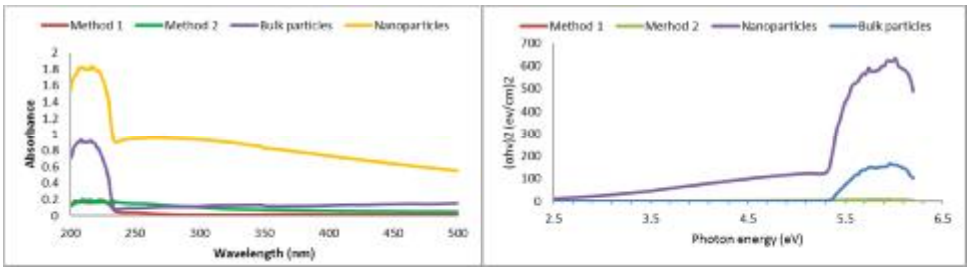

A B

Figure (10): (A) absorptions spectrum and (B) $(ahv)^2$ versus photon energy of green synthesis ZrO_2 NPs using *A. cepa* plant extract, data showed first and second methods compared with standard NPs and Bulk particles.

Green synthesis by *L. esculentum* plant extract : Sizes range, calculated by (AFM) were (50 - 150) and (50 - 145) nm with average diameter: 94.95 nm, 95.48 nm of first and second method respectively, (Figure 11 A). Roughness average (RA) and Root mean square (Sq) of first method was: 0.509 nm and 0.591 nm. While those of second were: 0.427 nm and 0.502 nm, respectively. Figure (11 B and C) showed AFM topographic images of green synthesis ZrO2 nanoparticles.

Figure (12) showed SEM image of ZrO_2 green synthesis NPs using first and second method of *L. esculentum*. Particle size were large than (80 and 90) nm respectively.

Figure (13) showed that results of FT-IR spectra, samples exhibited absorption peaks located near 380 (9) cm^{-1}, 420 (12) cm^{-1}, 580 (14) cm^{-1} and 620 (3)cm^{-1} which give an indication of presence Zr-O stretching bond.

XRD pattern of green synthesis NPs produced by first and second methods NPs showed the presence of five peaks of each of them. Strong diffraction peaks were: 28.292° (-111), 31.543° (111) and 34.279° (200) for first method and 28.179° (-111), 31.442° (111) and 24.073° (110) for second method, (Table 4). The average crystallite size of nanoparticles was calculated by Scherer's equation, they were 21.370 nm and 20.489 nm for first and second methods

respectively, (Figure 14). The results of all samples indicating that the structure were Baddeleyite crystalline.

The results of UV–visible spectral found that the absorption spectra of green synthesis ZrO_2 NPs exhibit strong absorption below 232 nm, 215 nm for first and second methods of green synthesis NPs compared with 215 nm in both standards synthetic NPs and bulk particles. The value of optical band gaps were about 5 eV and 3.4 eV for first and second methods of green synthesis NPs compared with 5.2 eV and 5.3 eV for standard synthetic NPs and bulk particles respectively, figure (15).

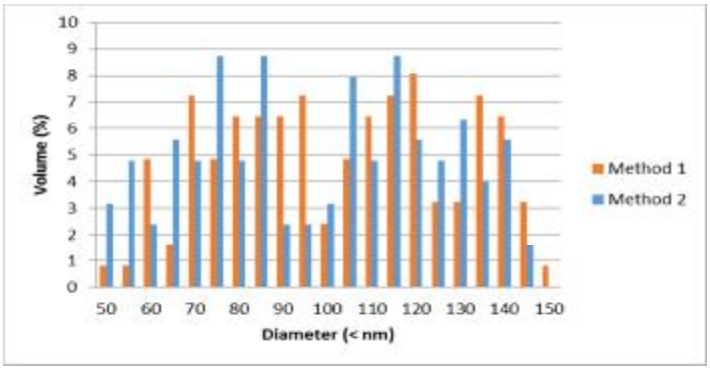

(A)

(B)

(C)

Figure (11): (A) Granularity volume distribution chart of ZrO_2 NPs synthesis by *Lycopersicon esculentum* plant extract using first and two methods, their average size were: 94.95 nm and 95.48 nm respectively. (B) and (C): AFM topographic images of first and two methods respectively.

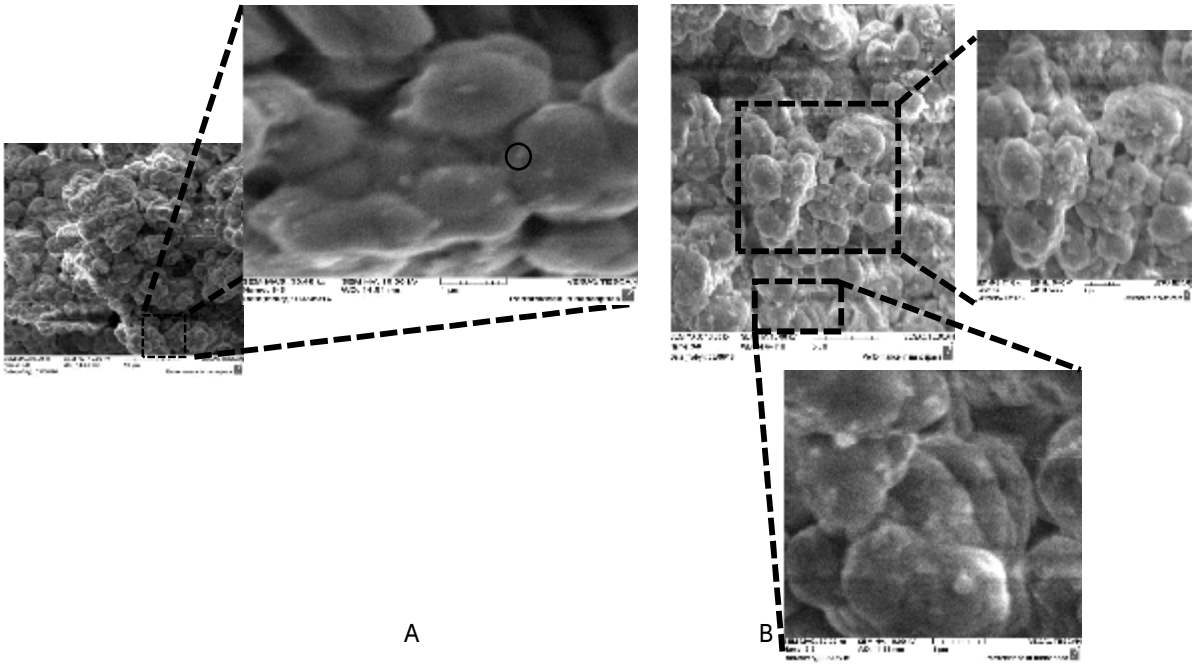

A B

Figure (12): SEM image of ZrO_2 green synthesis NPs using (A) first method, (>80 nm), and (B) second method, (>90 nm), of *L. esculentum*.

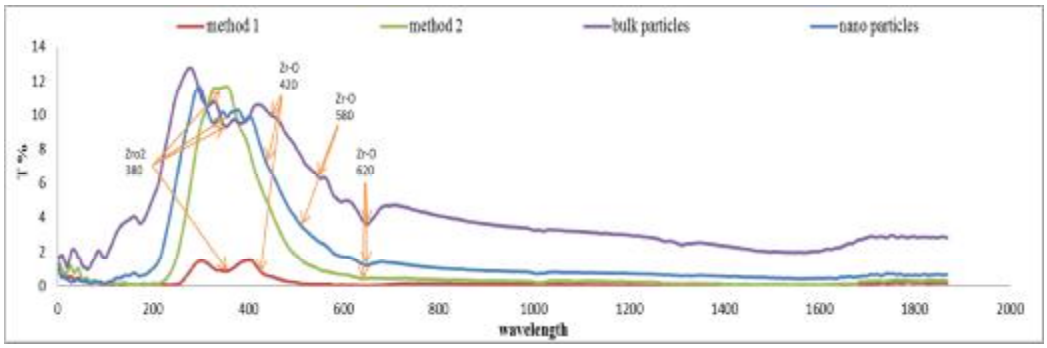

Figure (13): FT-IR spectra of ZrO_2 produced by the first and second methods *L. esculentum*.

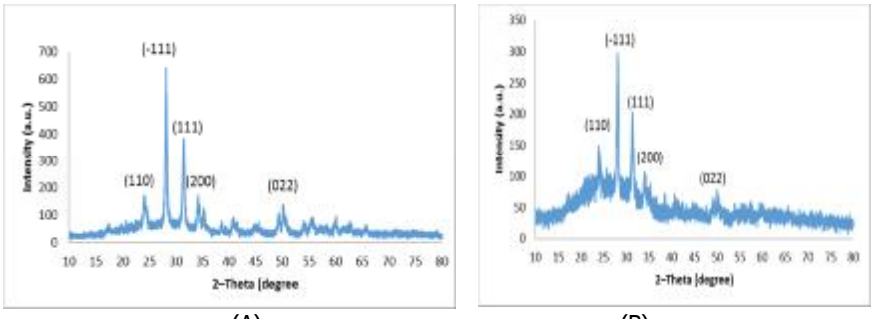

(A) (B)

Figure (14): X-ray pattern of ZrO_2 of: (A and B) green synthesis nanoparticles using first and second methods of *L. esculentum*. L. plant extract.

Table (4): Summary of X-ray characterization of ZrO_2 green synthesis nanoparticles synthesis by *L. esculentum* plant extracts compared with standard nanoparticles and bulk particles.

Sample	Planes (hkℓ)	Crystal shape	2 theta (DEG)	FWHM (DEG)	D (nm)	STRAIN XE-4	DIS X1014
Method 1	-111	Baddeleyite	28.292	0.349	23.366	59.318	18.317
	111	Baddeleyite	31.543	0.388	21.183	65.431	22.286
	200	Baddeleyite	34.279	0.423	19.563	70.847	26.129
Method 2	-111	Baddeleyite	28.179	0.381	21.397	64.776	21.843
	111	Baddeleyite	31.442	0.400	20.526	67.523	23.735
	110	Baddeleyite	24.073	0.413	19.544	70.915	26.179

(hkℓ) planes: crystallographic plane; FWHM : Full width at half maximum; D: dimension of Crystal in nm; η x10^{-4}: strain value; δ x 10^{14}: dislocation density; NPs: nanoparticles; BPs: particles.

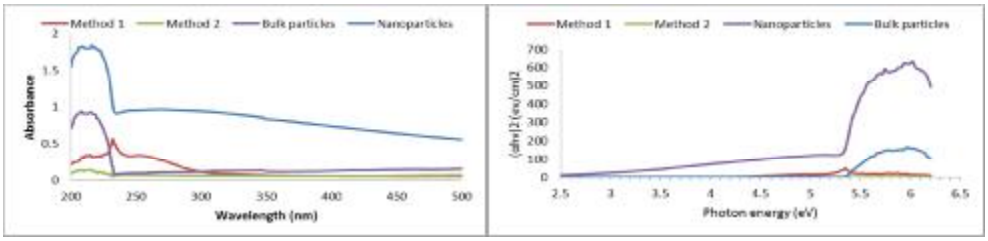

A B

Figure (15): (A) absorptions spectrum and (B) $(ahv)^2$ versus photon energy of green synthesis ZrO_2 NPs using *L. esculentum* plant extract, data showed first and second methods compared with standard NPs and Bulk particles.

These approach of using plants extracts for synthesis NPS have more benefits compared to usual techniques, physical and chemical, because of the availability of more constituents by biological bodies for the formation of nanostructures, (Narayanan *et al.*, 2011), it is an environment friendly approach because of its biocompatibility, clean and non-toxic which avoid adverse effects during their application, (Prathna *et al.*, 2010). Most bioprocesses occur under normal air pressure and temperature, reducing energy, inexpensive and high-yield, (Shaligram *et al.* 2009). The interesting properties of the plants is: that they are easily available, have fascinated the workers of its rapid, it provides a single step technique for the green synthesis process, broad variability of metabolites that aid in reduction, simple, stable, cost-effective method (Noruzi, 2015). The rate of production is faster than chemical and physical synthesis (Because of its ability to reduce the metal ions in a shorter time), (Padil *et al.*, 2013). Current results approved that *C. annum, A. cepa, L. esculentum*, plants extracts were an efficient routes to synthesis zirconium nanoparticles. The best plant extracts which produce ZrO2 was *A. cepa* fallowed by *C. annum,* this is based on the results of AFM which gave the size of particles. Current results is agree with the results of Sutradhar and others which reported the using of tomato extract as reducing agent for the synthesis of ZnO NPs of well-defined dimensions in bulk amount, (Sutradhar et al., 2015). These plants contain phytochemicals, such as: quercetin and its glycosides, phenolic acids, allicin in *A. cepa* and amine and aliphatic esters in *B. rapa* which were involved in the reduction and stabilization of silver nanoparticles, (Narayanan *et al.*, 2014), Betanin, betalains and betazanthins in *B. vulgaris,* (Sepúlveda-Jiménez *et al.*, 2004). These biomolecules could be used as bioreductants to react with metal ions and they may also be used as scaffolds to direct formation of nanoparticles, (Castro *et al.*, 2011).

Biological activities:

Antifungal activity of ZrO_2: The efficacy of antifungal in terms of zones of inhibition (mm) was measured against five different concentrations, (Table 5). In two species of Fusarium, which tested here, all green synthesis and standard nanoparticles showed good reductions of them but green synthesis nanoparticles were more reducer than standard NPs and *F. Moniliforme* was more sensitive to NPs compared with *F. graminearum*. Bulk particles were less effect on inhibition rate of both species compared with NPs.

Table (5): Comparison between the effect of green synthesis and standard NPs with bulk particles of ZrO_2 on Inhibition rate of *F. moniliforme* and *F. graminearum*.

Con.(mg/ml)	*F. Moniliforme*			*F. graminearum*		
	G. NPs	St. NPs	B. Ps	G. NPs	St. NPs	B. Ps
200	90.303	83.636	58.788	67.879	55.152	9.091
20	90.909	70.909	76.97	87.273	42.424	49.091
2	74.545	72.121	70.909	47.237	53.333	15.152
0.2	86.667	69.697	68.485	63.636	40.6606	30.303
0.02	89.697	75.152	73.333	61.818	56.364	23.636
CT-	0	0	0	0	0	0

Con.; concentrations; CT-: untreated fungi, G. NPs: green synthesis nanoparticles, St. NPs.: standard nanoparticles, B. Ps: bulk particles.

Generally, size of bulk particles is more than 2 micrometre, at these sizes it is difficult for them to inter cell membrane, so low size particles, like NPs, can inter cell membrane and cause different actions leading to death. Antifungal ability for the green synthesis ZrO2 nanoparticles may due to their large surface area and lower size. It can destroy ergosterol in fungal cells membrane (making various gradients between cytoplasmic membranes can keep their membrane potential ability) and it causes cell death because, (Allaker, 2010). Current results of antifungal effect of Zirconium oxide nanoparticles were compatible with the results of the results of Gowri and others in (2014) which proved inhibition effect of the green synthesis ZrO2 nanoparticles in treated cotton for hindering the growth of *C. albicans* and *A. niger* fungal strains, (Gowri *et al.*, 2014) . This study agrees with the positive results of Abdul Jalill and other in (2016b), they found that zirconium oxide nanoparticles can inhibit the fungal growth and sporulation and decrease pathogenicity of it but they have some negative effect on different parameters of plant growth, (Abdul Jalill *et al.*, 2016a).

Antibacterial activity of ZrO_2: Zirconium dioxide nanoparticles were tested for their antimicrobial efficacy against bacterial cultures of *E. coli* and *S. aruse* by well diffusion method. Five concentrations of ZrO_2 nanoparticles were used for the study. The results are shown in Table (6), which shows the highest bacterial Inhibition rate found in (200, 20 and 0.2 mg/ml) and (200 and 20 mg/ml) for *E. coli* and *S. aruse* respectively in all methods. Green synthesis NPs and Bulk particles were more effective than Standard NPs in *E. coli*. In the other hands, Green synthesis NPs and Standard NPs were more effective than Bulk particles in S. aruse, (Table 7). Moreover, the results showed that the ZrO2 NPs is more effective in *E. coli* than *S. aureus*.

Table (6): Comparison between the effect of green synthesis NPs and standard synthetic NPs with bulk particles of Zirconium oxide on Inhibition rate of *E. coli.*

Con. (mg/ml)	Methods (treatment/ nutrient broth)								
	2/2			2.5/1.5			3/1		
	G. NPs	St. NPs	B. Ps	G. NPs	St. NPs	B. Ps	G. NPs	St. NPs	B. Ps
200	100	97.197	98.258	99.091	92.727	96.288	97.348	92.121	98.258
20	99.091	92.727	96.288	98.712	95.152	99.47	94.242	97.803	95.303
2	85.227	87.576	97.955	86.364	96.591	94.848	85.909	95.379	90.455
0.2	86.742	76.515	91.667	99.091	93.712	98.03	96.667	95.303	96.894
0.02	87.5	90.833	85.758	87.121	92.879	96.742	89.773	90	98.182
CT-	0	0	0	0	0	0	0	0	0

Con.; concentrations; CT-: untreated, G.NPs: green synthesis nanoparticles, St. NPs.: standard nanoparticles, B. Ps: bulk particles.

Table (7): Comparison between the effect of standard NPs and green synthetic NPs with bulk particles of Zirconium oxide on Inhibition rate of *S. aureus*.

Con.(mg/ml)	Methods (treatment/ nutrient broth)								
	2/2			2.5/1.5			3/1		
	G. NPs	St. NPs	B. Ps	G. NPs	St. NPs	B. Ps	G. NPs	St. NPs	B. Ps
200	95.813	99.875	88.563	91.875	99.188	79.813	96.688	99.188	91.25
20	92.188	96.438	95.375	90	98.938	82.5	88.25	99.875	69.75
2	91.688	87.688	57.652	89.938	92.188	81.688	94.688	90.313	49.375
0.2	88.938	92.063	97.938	92.813	89.938	94.25	90.25	90.125	97
0.02	91.625	77.5	93.313	88.188	81.625	93.75	90.063	75.625	91.688
CT-	0	0	0	0	0	0	0	0	0

Con.; concentrations; CT-: untreated, G.NPs: green synthesis nanoparticles, St. NPs.: standard nanoparticles, B. Ps: bulk particles.

The antibacterial activities of current studies were probably depending on different factors such as:

1. Damage of cell membrane because the production of lactate dehydrogenase is increases according to, (Lin *et al.*, 2006), who study the effect of ZrO_2 on *Klebsiella sp*., *E. coli*, *Staphylococcus sp*. and *Salmonella*.
2. Or may due to accumulation or deposition on the surface of *S. aureus* cells, disorganization of *E. coli* membranes, which increases membrane permeability leading to accumulation of nanoparticles in the bacterial membrane and cytoplasmic regions of the cells, (Massodiyeh *et al.*, 2015) .
3. Surface modification, composition, intrinsic properties and the cell surface characteristics of microorganisms could be another reasons.
4. Nanoparticles may react with the thiol group (-SH) in the bacterial cell wall, allowing the transport of nutrients through the cell wall, inactivate the protein and decrease the cell permeability and eventually causing the cellular death, (Zhang *et al.*, 2009).
5. Decomposition of bacterial outer membranes by reactive oxygen species (ROS), primarily hydroxyl radicals (OH), which leads to phospholipid peroxidation, and ultimately cell death, (Jayaseelan *et al.*, 2013).
6. Deactivation of cellular enzymes and DNA, by coordinating to electron-donating groups such as thiols, carbohydrates, amides, indoles, hydroxyls etc, (Durairaj *et al.*, 2015).
7. Recently, it has been demonstrated that metal oxide nanoparticles exhibit excellent biocidal and biostatic action against Gram-positive and Gram-negative bacteria, (Goerne *et al.*, 2012), and Inhibition biofilm of S. aureus and *E. coli*, Bacillus subtilis, Pseudomonas aeruginosa, nanoparticles inhibited growth of gram-positive by 90% but gram-negative was much more resistant, (Adams *et al.*, 2006).

Effect on some seeds germination parameters of *B. vulgaris var. vulgaris* and *E. sativa*: In *B. vulgaris var. vulgaris*, (Table 8), all concentrations of green synthesis nanoparticles reduced GP, MGT, MDG, GV and PI but they increased GR compared with control. The same results found using standard NPs except the GR (2mg/ml) and GV (20-200) mg/ml and 2mglml in PI which were vs. versa while bulk particles were reduced GP, MGT and MDG but they increased GR and PI (except 20 mg/ml). In *E. sativa*, most concentrations of: green synthesis nanoparticles, standard NPs and bulk particles reduced GP, MGT, MDG, GV and PI but they increased GR compared with control, (Table 9).

In this study, green synthesis NPs and standard NPs reduced some seed germinations parameters such as GP, MGT, MDG, GV and PI at the time they increased GR compared with control. This is may be due to inhibited activities of hydrolytic enzymes by large or small size particles of minerals, (Hunter *et al*., 2011). For reduction by bulk particles, it is probable that increasing the concentration of bulk induced aggregation of particles and resulted in clogging of pores that interrupted water uptake by seeds. Stimulate growth for NPs of current study may be due to several reasons: the increasing essential metal nutrient uptake reported to enhances the plant development, (Khot *et al.*, 2012); (Fraceto *et al.*, 2016), or NPS, perhaps, have helped the water absorption by the seeds.

Conclusions and Recommendations

Capsicum annum Allium cepa and *Lycopersicon esculentum* could be used to green synthesis ZrO_2

NPs. All nanoparticles were in nano size with well optical properties. Crystal's shapes were Baddeleyite. Both of green synthetic and standard NPs of ZrO_2 had good antifungal and antibacterial activity compared with bulk particles which were less effect. ZrO_2 NPs had negative effects on seed germinations and other growth parameters of *B. vulgaris* and *E. sativa* such as reductions in GP, MGT, MDG, GV and PI but they increased GR. Fresh extract of some medical plants can be used for green synthesis nanoparticles with analyse them to detect active chemical compositions would be benefit. Optimized other conditions for synthesis NPs such as: PH, charged, pressure and light, exposure time.

Acknowledgments

The authors would like to thank Al-Mustansiriyah University (www. uomustansiriyah.edu.iq) Baghdad Iraq for its support in the present work.

References

Abdul Jalill, R.DH.; Nuaman, R.S. and Abd, A.N. 2016a. Biological synthesis of Titanium Dioxide nanoparticles by *Curcuma longa* plant extract and study its biological properties. WSN. 49(2) 204-222.

Abdul Jalill, R.DH. and Nuaman, R.S. 2016b. Silver nitrate and zirconium oxide nanoparticles as management of wheat damping-off caused by *Fusarium graminearum*. J. Genet. Environ. Resour. Conserv., 4(2): 85-93.

Adams, K.L.; Lyon, Y.D. and Alvarez, J.J.P. 2006. Comparative eco-toxicity of nanoscale TiO2, SiO2, and ZnO water suspensions. Water Res., 40: 3527-3532.

AL-Kaisi, W.A., Muhsen, T.A.A., Hamed, A.S. 2011. Effect of mycorrhiza (*Glomus mosseae*) and superphosphate on physiological characters of *Hodeum vulgare*, College of Basic Education J., 72: 765-784.

Allaker, R.P.; Vargas-Reus, M.A. and Ren. G.G. Nanometal a metals as antimicrobials. Chapter 13 (327 p.). In: Lagaro´ N, J. M.; Ocio, M. J. and Lo´pez-rusbio, A. 2012. Antimicrobial polymers. John Wiley & Sons, Inc., Hoboken, New Jersey Published simultaneously in Canada. 596 p.

Ba-Abbad, M.M.; Kadhum, A.H.; Mohamad, A.B.; Takriff, M.S. and Sopian, K. 2012. Synthesis and catalytic activity of TiO_2 nanoparticles for photochemical oxidation of concentrated chlorophenols under direct solar radiation. Int. J. Electrochem. Sci. 7: 4871– 4888.

Booth, C. (1977). Fusarium, Laboratory Guide to the Identification of the Major Species. Commonwealth Mycological Institute, Kew, Surrey, England, 58 pp.

Chandra, N.; Singh, D.K.; Sharma, M.; Upadhyay, R.K.; Amritphale, S.S. and Sanghi, S.K. (2010). Synthesis and characterization of nano-sized zirconia powder synthesized by single emulsion-assisted direct precipitation, J. Colloid Interface Sci., 342: 327-332.

Castro, L.; Blazquez, M.L.; Munoz, J.A.; Gonzalez, F.; Garcıa-Balboa, C.; Ballester, A. (2011). Biosynthesis of gold nanowires using sugar beet pulp. Process Biochem. 46: 1076–1082.

Cullity, B.D. (1978.). Elements of X-ray Diffraction, IInd Ed, Addison Wesley, London.

De, D.; Mandal, S.M.; Gauri, S.S.; Bhattacharya, R.; Ram, S. and Roy, S.K. (2010). Antibacterial effect of lanthanum calcium manganite (La0.67Ca0.33MnO3) nanoparticles against *Pseudomonas aeruginosa* ATCC 27853. J. Biomed. Nanotechnol., 6(2):138–144.

Durairaj, P.; Malla, S.; Nadarajan, S.P.; Lee, P-G.; Jung, E.; Park, H.H.; Kim, B-G. and Yun, H. 2015. Fungal cytochrome P450 monooxygenases of *Fusarium oxysporum* for the synthesis of ω-hydroxy fatty acids in engineered *Saccharomyces cerevisiae*. Microb. Cell Fact. 14:45. doi: 10.1186/s12934-015-0228-2.

Eugenio, M.; Müller, N.; Frasés, S.; Almeida-Paes, R.; Maurício L.; Lima, T. R.; Lemgruber, L.; M.; Farina, Souza, W.; and Anna, C. S. 2016. Yeast-derived green synthesis of silver/silver chloride nanoparticles and their antiproliferative activity against bacteria. RSC Adv., 6: 9893-9904.

Fraceto, L.F.; Grillo, R.; Medeiros, G. A.; Scognamiglio, V.; Rea, G. and Bartolucci, C. 2016. Nanotechnology in Agriculture: which innovation potential does it have? Front Environ. Sci., 4: 1-5.

El-Said, W.A.; Cho, H.; Yea, C. and Choi, J. 2014. Synthesis of metal nanoparticles inside living human cells based on the intracellular formation process. Advanced Materials. 26 (6): 910–918.

Feizi, H.; Moghaddam, R.P.; Shahtahmassebi, N. and Fotovat, A. 2012. Impact of bulk and nanosized titanium dioxide (TiO_2) on wheat seed germination and seedling growth. Biological Trace Element Res., 146(1): 101-106.

Goerne, T.M.L.; Lemus, M.A.A.; Morales, V.A. ; López, E.G. and Ocampo, P.C. 2012. Study of bacterial sensitivity to Ag-Tio2 nanoparticles. J. Nanomed. Nanotechol., S5: 003.

Table (8): Comparison between the effect of standard nanoparticles and green synthetic nanoparticles with bulk particles of Zirconium oxide on some seeds germination parameters of *B. vulgaris var. vulgaris*.

Con. (mg/ml)	% GP			% GR			MGT			MDG			GV			PI		
	G. NPs	St. NPs	BPs	G. NPs	St. NPs	BPs	G. NPs	St. NPs	BPs	G. NPs	St. NPs	BPs	G. NPs	St. NPs	BPs	G. NPs	St. NPs	BPs
200	74	68	70	0.78	0.68	0.72	11.2	10.8	10.9	740	680	700	991.67	930	816.67	2.7	2.7	2.15
20	62	80	86	0.64	0.94	1.32	11	13.6	11.6	620	800	860	726.67	1170	1276	1.85	3.3	3.3
2	64	62	70	0.65	0.41	1.08	11	12.6	9.5	640	620	700	724	526.67	1000	2.55	1.6	4
0.2	60	86	70	0.68	0.76	1.29	11.8	12.3	8.7	600	680	700	476	793.33	1500	1.8	1.55	4.1
0.02	76	70	74	1.11	1.05	1.18	12	10.9	9.6	760	700	740	828.33	1088	1036	2.85	2.55	3.1
ct-	90	90	90	0.64	0.64	0.64	21.3	21.3	21.3	900	900	900	910	910	910	2.7	2.7	2.7

Data shows means; Con.: concentration; CT-: untreated; G.NPs: green synthesis nanoparticles; St. NPs.: standard nanoparticles; B. Ps: bulk particles.GP: Germination percentage; GR: Germination rate; MGT: Mean germination time; MDG: mean daily germination; GV: Germination Value; PI: Promoter Indicator.

Table (9): Comparison between the effect of standard nanoparticles and green synthetic nanoparticles with bulk particles of Zirconium oxide on some seeds germination parameters of *E. sativa*.

Con. (mg/ml)	% GP			% GR			MGT			MDG			GV			PI		
	G. NPs	St. NPs	BPs	G. NPs	St. NPs	BPs	G. NPs	St. NPs	BPs	G. NPs	St. NPs	BPs	G. NPs	St. NPs	BPs	G. NPs	St. NPs	BPs
200	90	72	66	3.77	1.38	1.26	6.1	8.6	5.4	1100	720	660	7980	1770	1810	1.5	4.8	3.75
20	80	88	80	3.09	2.96	2.70	5.6	7.6	6.9	800	880	800	4360	4280	3400	2.35	2.3	2.95
2	82	90	84	3.32	3.58	3.65	5.7	6.1	5.7	820	900	840	4960	5820	6020	1.900	2	0.6
0.2	44	84	88	1.26	3.13	3.93	4.0	6.6	5.1	440	840	880	1280	4780	6540	1.950	1.55	1.4
0.02	82	74	82	3.47	3.27	2.90	5.5	4.5	6.4	820	740	820	5360	4760	4420	0.150	0.8	2.95
ct-	96	96	96	1.24	1.24	1.24	13.6	13.6	13.6	960	960	960	1803.33	1953.33	1803.33	3.80	3.8	3.8

Data shows means; Con.: concentration; CT-: untreated; G.NPs: green synthesis nanoparticles; St. NPs.: standard nanoparticles; B. Ps: bulk particles.GP: Germination percentage; GR: Germination rate; MGT: Mean germination time; MDG: mean daily germination; GV: Germination Value; PI: Promoter Indicator.

Goh, P.S.; Ng, B.C.; Lau, W.J. and Ismail, A.F. 2015. Inorganic nanomaterials in polymeric ultrafiltration membranes for water treatment. Purific. Revie., 44: 216–249.

Gowri, S.; Gandhi, R.R. and Sundrarajan, M. 2014. Structural, optical, antibacterial and antifungal properties of zirconia nanoparticles by biobased protocol. J. Mater. Sci. Technol., 30(8): 782e790.

Hunter, L. W.; Shiekh, F. A.; Pisimisis, G. T.; Kim, S.; Edeh, S. N.; Miller, V. M.; and Lieske J. C. 2011. Key role of alkaline phosphatase for development of human-derived nanoparticles *In vitro.* Acta Biomater., 7(3): 1339–1345.

Huang, L.; Cao, Z.; Meyer, H.M.; Liaw, P.K.; Garlea, E.; Dunlap; J.R.; Zhang, T. and He, W. 2011. Responses of Bone-Form Cells on Pre-Immersed Zr-Base Bulk Metallic Glasses: Effect of Composition and Roughness. Acta Bio-mater., 7: 395-405.

Ingale, A. G. and Chaudhari, A. N. 2013. Biogenic synthesis of nanoparticles and potential applications: an eco-friendly approach. Journal of Nanomedicine and Nanotechnol., 4(2).

Jayaseelan, C.; Rahuman, A.A.; Roopan, S.M. ; Kirthi, A.V. ; Venkatesan, J.; Kim, S.; Iyappan, M. and Siva, C. 2013. Biological approach to synthesize TiO_2 nanoparticles using Aeromonas hydrophila and its antibacterial activity. Spectrochimica Acta Part A. Molec. Biomol. Spectrosco., 107: 82–89.

Jobst, P.J.; Stenzel, O.; Schürmann, M. ; Modsching, N. ; Yulin, S.; Wilbrandt, S.; Gäbler, D.; Kaiser, N.; and Tünnermann, A. 2013. Optical properties of unprotected and protected sputtered silver films: Surface morphology vs. UV/VIS reflectance. Adv. Opt. Techn., 3: 91-102.

Joshi, P.; Chakraborti, S.; Chakrabarti, P.; Haranath, D.; Shanker, V.; Ansari, Z A. ; Singh, S P. and Gupta, V.J. 2010. Role of surface adsorbed anionic species in antibacterial activity of ZnO quantum dots against *Escherichia coli*. Nanosci. Nanotechnol., 9: 6427-6433.

Kalyani, P.; Vineela, K. C.; Geetha, S.; and Hemalatha, K.P.J. 2016. Green synthesis of silver nano particles from *Aspergillus niger* (MTCC-961). Int. J. Curr. Microbiol. App. Sci., 5(10): 50-56.

Kelsall, R.W.; Hamley, I.W. and Geoghegan, M. 2005. Nanoscale science and technology. John Wiley and Sons Ltd, 473p.

Khot, L.R.; Sankaran, S.; Maja, J.M.; Ehsani, R. and Schuster, E.W. 2012. Applications of nanomaterials in agricultural production and crop protection: a review. Crop Prot., 35: 64-70.

Kratošová, G.; Vávra, I.; Horská, K.; Životský, O.; Němcová, Y.; Bohunická, M.; Slabotinskú, J.; Rosenbergová, K.; Kadilak, A.; and Schröfe, A. 2013. Synthesis of metallic nanoparticles by diatoms and chrysophytes - prospects and applications. Chapter 5 (Page no: 61). In: Rai, M., Posten, C. Green synthesis of nanoparticles: mechanisms and applications. CAB eBooks. DOI: 10.1079/9781780642239.0000.

Lin, W.; Yue-wern, H.; Xiao-Dong, Z. and Ma, Y. 2006. Toxicity of Cerium Oxide Nanoparticles in Human Lung Cancer Cells. Int. J. Toxicol., 25(6): 451-457.

Marchiol, L.; Mattiello, A. and Poscic, F. Giordano, C.; Musetti, R. 2014. *In vivo* synthesis of nanomaterials in plant: location of silver nanoparticles and plant metabolism. Nanoscale Res Lett. 9(1):101. doi: 10.1186/1556-276X-9-101.

Massodiyeh, F.; Karimi, J.; Khanchi, A. R. and Mozdianfard, M.R. 2015. Zirconia nanoparticle synthesis in sub and supercritical water-particle morphology and chemical equilibrium. Powder Technol., 269:461-8.

Meshram, R.S.; Suryavanshi, B.M. and Thombre, R.M. 2012. Structural and optical properties of CdS thin films obtained by spray pyrolysis. Adv. Appl. Sci. Res., 3: 1563–1571.

Narayanan, K.B. and Sakthivel, N. 2011. Green synthesis of biogenic metal nanoparticles by terrestrial and aquatic phototrophic and heterotrophic eukaryotes and biocompatible agents. Adv Colloid Interface Sci. 169: 59-79.

Naveen, H. K.S.; Gaurav Kumar.; Karthik L.; and Bhaskara Rao K.V. 2010. Extracellular biosynthesis of silver nanoparticles using the filamentous fungus *Penicillium sp*. Arch. Appl. Sci. Res., 2(6): 161-167.

Nimare, P. and Koser, A.A. 2016. Biological synthesis of ZrO_2 nanoparticle using *Azadirachta indica* leaf extract. IRJET, 2395 -0056.

Njagi, E.C.; Huang, H.; Stafford, L.; Genuino, H.; Galindo, H.M.; Collins, J.B.; Hoag, G.E. and Suib, S.L. 2011. Bio synthesis of iron and silver nanoparticles at room temperature using aqueous sorghum bran extracts. Langmuir, 27(1): 264–271.

Noruzi, M. 2015. Biosynthesis of gold nanoparticles using plant extracts. Bioprocess Biosyst. Eng., 38: 1-14.

Padil, V.V.T and Černík, M. 2013. Green synthesis of copper oxide nanoparticles using gum karaya as a biotemplate and their antibacterial application. Int. J. Nanomed., 8: 889–898.

Plaza, D. O.; Gallardo, C.; Straub, Y. D.; Bravo, D. and Pérez-Donoso, J. M. 2016. Biological synthesis of fluorescent nanoparticles by cadmium and tellurite resistant Antarctic bacteria: exploring novel natural nanofactories. Microbial. Cell Factories, 15:76. DOI: 10.1186/s12934-016-0477-8.

Prathna, T.C.; Mthew, L.; Chandrasekaran, N.; Raichur, A. M. and Mukherjee, A. 2010. Biomimetic synthesis of nanoparticles: science, technology and applicability, Biomimetics-Learning from Nature, 1-20.

Raveendran, P.; Fu, J. and Wallen, S.L. 2003. Completely green synthesis and stabilization of metal nanoparticles. J. Am. Chem. Soc., 125: 13940-13941.

Seabra, A. B. and Durán, N. 2015. Nanotoxicology of metal oxide nanoparticles. Metals, 5: 934-975. doi: 10.3390/met5020934.

Sepúlveda-Jiménez, G.; Rueda-Benítez, P.; Porta, H. and Rocha-Soda, M. 2004. Betacyanin synthesis in red beet (*Beta vulgaris*) leaves induced by wounding and bacterial infiltration in preceded by an oxidative burst. Physiol. Mol. Plant Pathol., 64:125–133.

Siddiqi, K. S. and Husen, A. 2016. Fabrication of metal oxide nanoparticles by algae and their toxic effects. Nanoscale Res. Lett., 11:363.

Shaligram, N.S.; Bule, M.; Bhambure, R.M.; Singhal, R.S.; Singh, S.K.; Szakacs, A. and Pandey, A. 2009. Biosynthesis of silver nanoparticles using aqueous extract from the compactin producing fungal strain. Proce. Biochem., 44:939–948.

Suresh, V. and Jaikumar, S. Arunachalam, G. 2010. Antidiabetic activity of ethanolic extract of stem bark of *Nyctanthes arbortristis* Linn. Res. J. Pharmace. Biol. Chem. Sci., 1(4): 311-317.

Sutradhar, P. and Saha, M. 2016. Green synthesis of zinc oxide nanoparticles using tomato (*Lycopersicon esculentum*) extract and its photovoltaic application. J. Exper. Nanosci., 11: 314–327.

Wei, W.; Mao, X.; Ortiz, L.A. and Sadoway, D.R. 2011. Oriented silver oxide nanostructures synthesized through a template-free electrochemical route. J. Mater. Chem., 21 (2): 432–438.

Zhang, H. and Chen, G. 2009. Potent antibacterial activities of Ag/TiO_2 nanocomposite powders synthesized by a one-ppot sol-gel method. Environ. Sci. Technol., 43(8): 2905-2910.